Research Article | Vol. 26, No. 11 | 28 May 2018 | OPTICS EXPRESS 14010

Optics EXPRESS

Model of radial basis functions based on surface slope for optical freeform surfaces

KAINIAN TONG,[1] YI ZHENG,[1] ZAN ZHANG,[1] XING ZHAO,[1,2,*] BO ZHANG,[1] LIPEI SONG,[1] LINGJIE WANG,[3] CHAO WANG,[3] AND PENGFEI WU[1,2]

[1]*Institute of Modern Optics, Nankai University, Tianjin 300350, China*
[2]*Tianjin Key Laboratory of Optoelectronic Sensor and Sensing Network Technology, Tianjin 300350, China*
[3]*Key Laboratory of Optical System Advanced Manufacturing Technology, Changchun Institute of Optics, Fine Mechanics and Physics, Chinese Academy of Sciences, Changchun 130033, China*
[*]*zhaoxingtjnk@nankai.edu.cn*

Abstract: The model fitting degree of optical freeform surfaces is of utmost design importance. We develop a model with radial basis functions based on the surface slope (RBF-slope) for optical freeform surfaces with asymmetric structures. The RBF-slope model improves the basis-function distribution for circular apertures and establishes a relationship between shape factor and local surface slope, which provides the model with better fitting ability than the conventional RBF model (RBF-direct); fitting experiments for off-axis conic surfaces, "bumpy" paraboloids, and the design of a single mirror magnifier demonstrate the efficacy of our approach. Our method can effectively improve aberration balancing of optical freeform surfaces, resulting in high-quality imaging.

OCIS codes: (000.3860) Mathematical methods in physics; (080.2740) Geometric optical design.

References and links

1. X. Hu and H. Hua, "High-resolution optical see-through multi-focal-plane head-mounted display using freeform optics," Opt. Express **22**(11), 13896–13903 (2014).
2. C. Xu, D. Cheng, J. Chen, and Y. Wang, "Design of all-reflective dual-channel foveated imaging systems based on freeform optics," Appl. Opt. **55**(9), 2353–2362 (2016).
3. E. Muslimov, E. Hugot, W. Jahn, S. Vives, M. Ferrari, B. Chambion, D. Henry, and C. Gaschet, "Combining freeform optics and curved detectors for wide field imaging: a polynomial approach over squared aperture," Opt. Express **25**(13), 14598–14610 (2017).
4. Z. Feng, L. Huang, G. Jin, and M. Gong, "Designing double freeform optical surfaces for controlling both irradiance and wavefront," Opt. Express **21**(23), 28693–28701 (2013).
5. T. Yang, J. Zhu, X. Wu, and G. Jin, "Direct design of freeform surfaces and freeform imaging systems with a point-by-point three-dimensional construction-iteration method," Opt. Express **23**(8), 10233–10246 (2015).
6. S. Sorgato, R. Mohedano, J. Chaves, M. Hernández, J. Blen, D. Grabovičkić, P. Benítez, J. C. Miñano, H. Thienpont, and F. Duerr, "Compact illumination optic with three freeform surfaces for improved beam control," Opt. Express **25**(24), 29627–29641 (2017).
7. V. F. Zernike, "Beugungstheorie des schneidenver-fahrens und seiner verbesserten form, der phasenkontrastmethode," Physica **1**(7), 689–704 (1934).
8. R. J. Noll, "Zernike polynomials and atmospheric turbulence," J. Opt. Soc. Am. **66**(3), 207–211 (1976).
9. K. Fuerschbach, J. P. Rolland, and K. P. Thompson, "A new family of optical systems employing φ-polynomial surfaces," Opt. Express **19**(22), 21919–21928 (2011).
10. G. W. Forbes, "Shape specification for axially symmetric optical surfaces," Opt. Express **15**(8), 5218–5226 (2007).
11. G. W. Forbes, "Characterizing the shape of freeform optics," Opt. Express **20**(3), 2483–2499 (2012).
12. I. Kaya, K. P. Thompson, and J. P. Rolland, "Comparative assessment of freeform polynomials as optical surface descriptions," Opt. Express **20**(20), 22683–22691 (2012).
13. I. Kaya, K. P. Thompson, and J. P. Rolland, "Edge clustered fitting grids for φ-polynomial characterization of freeform optical surfaces," Opt. Express **19**(27), 26962–26974 (2011).
14. O. Cakmakci, S. Vo, H. Foroosh, and J. Rolland, "Application of radial basis functions to shape description in a dual-element off-axis magnifier," Opt. Lett. **33**(11), 1237–1239 (2008).
15. O. Cakmakci, B. Moore, H. Foroosh, and J. P. Rolland, "Optimal local shape description for rotationally non-symmetric optical surface design and analysis," Opt. Express **16**(3), 1583–1589 (2008).
16. O. Cakmakci, I. Kaya, G. E. Fasshauer, K. P. Thompson, and J. P. Rolland, "Application of radial basis functions to represent optical freeform surfaces," Proc. SPIE **7652**, 76520A (2010).

#327997 https://doi.org/10.1364/OE.26.014010
Journal © 2018 Received 11 Apr 2018; revised 10 May 2018; accepted 13 May 2018; published 16 May 2018

Optics EXPRESS

17. M. Maksimovic, "Optical design and tolerancing of freeform surfaces using anisotropic radial basis functions," Opt. Eng. **55**(7), 071203 (2016).
18. X. Lin, X. G. Liu, Y. Li, and G. Wei, "A new orbit fitting algorithm of space-borne SAR based on householder transformation," in Synthetic Aperture Radar, 2009. Apsar 2009. Asian-Pacific Conference (2009), pp. 832–835.

1. Introduction

Optical freeform surfaces, which have no rotational invariance, arbitrary shapes, and regular/irregular global structures, offer more degrees of design freedom than traditional optical surfaces such as spherical and conic surfaces, therefore leading to enhanced aberration control ability, high optical performance, multi-function to a single component and less number of elements. They have great advantages in both optical imaging systems [1–3] and non-imaging systems [4–6]. When designing optical systems with optical freeform surfaces, it is necessary to describe and characterize the freeform surface with a surface model based on certain kinds of polynomials. Because different freeform surface models have different fitting features, in order to compensate for complicated aberrations, it is critical to determine a suitable model to accurately characterize the freeform surface. The Zernike polynomial [7] model is considered as one of the popular models that characterize the sag of optical freeform surfaces. Zernike polynomials, which are a polynomial sequence orthogonal on the unit circular disk and closely related to the Seidel aberration, have been widely used in the fields of surface characterization, optical design, and optical testing [8,9]. Q-type polynomial model is becoming a practical model for optical freeform surface application because it offers a rough interpretation of the shape at a glance and facilitates a range of estimates of manufacturability [10,11]. The common feature of the Zernike polynomial and Q-type polynomial models are that they are both global-type models. This means that when they are used to fit a surface, any changes of the coefficient of any term in the polynomial will influence the sag value of the whole aperture. This leads to deterioration of fitting performance for complicated or asymmetric surfaces, and thus more terms of polynomial or special sample grids distribution is needed for a satisfactory performance [12,13]. To get a better characterization of freeform surface, Gaussian radial basis function (RBF) model was first proposed and applied in the design of the head-worn display (HWD) systems by Cakmakci et al. [14,15]. The highlight of the model, named as the RBF-Direct model in the literature, is that it has local surface fitting ability. This means that the change in aperture scope induced by variation of any term in the polynomial is limited, thereby leading to better model performance in fitting surfaces with strong local variations, which are often used to balance large aberrations in asymmetric systems. This has been proved in the design of single-element HWD systems, which have an off-axis magnifier characterized by the RBF-Direct model [15].

Although RBF-Direct model outperforms other freeform surface models such as the Zernike polynomial model, it still suffers from certain drawbacks. For example, in the design of the single-element HWD system illustrated in the literature [16], as shown in Fig. 1(a), the off-axis magnitude of the incident rays reflected by the upper part of the mirror is obviously larger than that of the rays reflected by the other parts, when the axis of the reflecting mirror is taken as optical axis. Then the upper part of the mirror need to be more sophisticated to compensate for larger and more complicated aberrations than the other parts, thus asymmetric features may be introduced to the mirror surface. Consequently, the description of the upper part of the mirror surface has to be sufficiently accurate to characterize this surface. However, because the basis functions of the RBF-Direct model have inefficient distribution and identical shape factors, the accuracy of characterization of this asymmetric surface is limited. This in turn reduces the potential aberration-balancing ability of the surface, as demonstrated by the lower image quality in Fig. 1(b) when X (the field of view, FOV) > 0 (corresponding to the upper part of the mirror). This means that surface characterization by the RBF-Direct model is not sufficiently accurate to compensate for optical aberrations. Therefore, it is of great importance to establish a more flexible RBF model to better represent complicated or asymmetric surfaces. Adaptive grid refinement method, which refines the local distribution of RBF until the global error is below the specified value, shows an improved fitting ability when fitting complicated surfaces [17]. However, this method will be computationally expensive and time-comsuming because of the self-adaptive process. In this paper, we propose a new RBF model that establishes the relationship between the shape factor and the surface shape without complex and repeated computation. Varying shape factors over the whole aperture add the flexibility of RBF model.

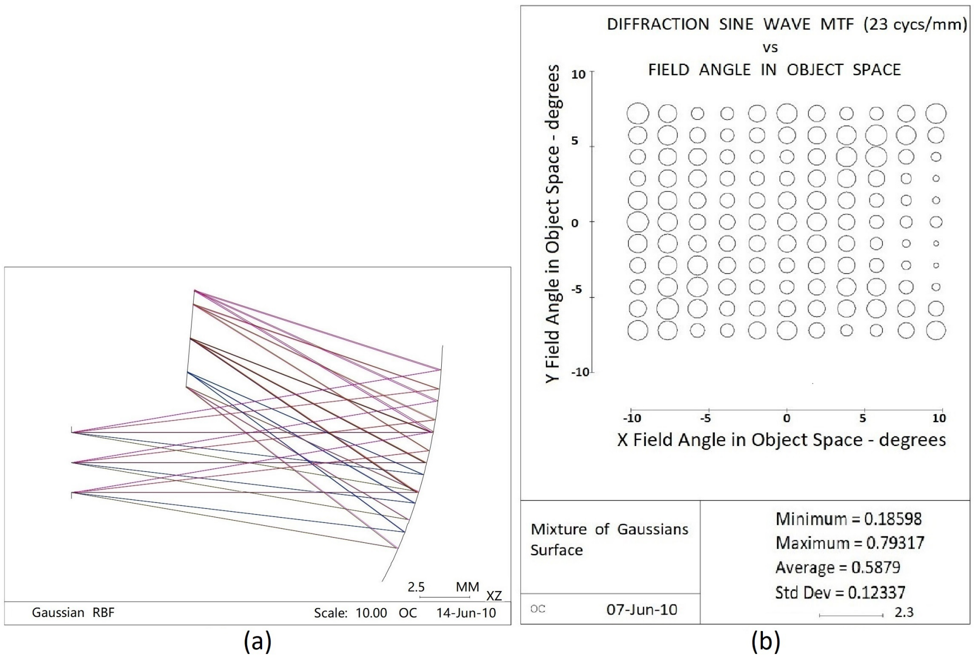

Fig. 1. (a) The geometry of single mirror magnifier (Ref [16], Fig. 3) (b) Modulation transfer function (MTF) at 23 cycles/mm for the 0-degree (radial) orientation of the single mirror magnifier where the surface was described with a 17 × 17 Gaussian radial basis function (RBF) (Ref [16], Fig. 4) (Text within these Figures has been modified for legibility).

The remainder of this paper is organized as follows: Section 2 introduces the process of establishing the new RBF model and summarizes the two principles underlying this RBF model. Section 3 compares the fitting precision of two kinds of RBF (RBF-Slope and RBF-Direct) models for an off-axis paraboloid. In Section 4, we take a paraboloid with large variation as a test surface and further compare the fitting ability of the two RBF models for this surface. Then the RBF-Slope and RBF-Direct models are applied to the design of a single mirror magnifier (Section 5) and the optical performances of these two models are compared and analyzed.

2. RBF-slope model

2.1 RBF-direct model

A freeform optical surface can be represented by a linear combination of RBFs added to a base conic as

Optics EXPRESS

$$
\begin{aligned}
z(x,y) &= \frac{c(x^2+y^2)}{1+\sqrt{1-(1+k)c^2(x^2+y^2)}} + \sum_i w_i \varphi_i(\| \vec{r} - \vec{r}_i \|) \\
&= \frac{c(x^2+y^2)}{1+\sqrt{1-(1+k)c^2(x^2+y^2)}} + \sum_i w_i e^{-\varepsilon_i^2((x-x_{0i})^2+(y-y_{0i})^2)},
\end{aligned} \tag{1}
$$

where z(x, y) denotes the sag of the freeform surface in the aperture, c is the vertex curvature, and (x, y) are the cartesian coordinates. The second term represents the combination of RBF $\varphi_i(\| \vec{r} - \vec{r}_i \|)$, where $\vec{r}$ denotes a vector pointing to any location in the aperture, $\vec{r}_i$ the vector pointing to the center of the RBF, $\| \cdot \|$ the Euclidean norm with w_i denoting the coefficients. Function φ_i can typically take the Gaussian form, as indicated in the second form of the equation. The use of the Gaussian function offers the following advantages: smoothness, approximate local characteristics (the value of Gaussian function rapidly reduces with increase in the distance away from the center), and good analyticity of solution [15]. Parameter (x_{0i}, y_{0i}) and shape factor ε_i determine the center position and the width of the basis function respectively. According to the approximate local properties of Gaussians, shape factor ε_i of each basis function determines the influence range of the basis function; larger shape factor induces smaller range and sharper basis function. This local property of the basis function sequence distributing throughout the aperture enables the Gaussian RBF a higher fitting ability than the Zernike polynomial, which leads to more advantages of the RBF model for characterizing asymmetrical optical freeform surfaces.

In the RBF-Direct model mentioned in [14–16], the distribution of the center (x_{0i}, y_{0i}) over the aperture is always uniform. For a circular aperture, the distribution of centers is shown in Fig. 2(a). Because the value of Gaussian function $\varphi_i(x,y)$ reduces with the increase of the distance between point (x, y) and center (x_{0i}, y_{0i}), the basis functions, whose centers locate outside the aperture, negligibly influence the surface region within the circular aperture. Moreover, the shape factors of all basis functions in the RBF-Direct model are set to be identical, which means that every function has the same amount of influence on the surface sag. With identical shape factors, only the change of the coefficients of the basis can contribute to the characterization of the surface in optical design, which strongly restricts the RBF model's ability to characterize asymmetrical freeform surfaces with large fields. Thus, in order to improve the characterizing ability of the conventional RBF-Direct model, we propose a RBF model based on the surface slope (RBF-Slope) in this study.

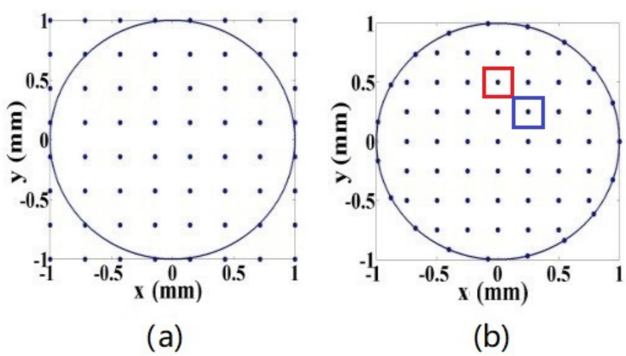

Fig. 2. Distribution comparison of basis functions between (a) RBF-Direct and (b) RBF-Slope models.

2.2 RBF-slope model

The RBF-Slope model follows two principles that are related to the distribution of the centers and the shape factor. The first principle is that all the centers of the basis function sequence are distributed within the aperture. For a rectangular aperture, the first criterion can be easily satisfied. For a circular aperture, the centers outside the aperture can be uniformly arranged around the edge of the aperture to ensure that every basis function affects the sag of the target surface, as shown in Fig. 2(b).

The second principle is that the shape factor ε_i is determined by the slope of the surface around the corresponding basis function center (x_{0i}, y_{0i}). When the basis functions are distributed over the aperture, the aperture can be divided into several square units, and the centers of these units coincide with the centers of basis functions. The number of these units is the same as the number of basis functions. The side length of each unit equals to the distance between two adjacent basis functions. Two units are marked with different colors in Fig. 2(b) for a better understanding of the unit. Then the shape factor ε_i of each basis function is set to be proportional to the peak-to-valley value of the surface sag in corresponding unit, so that the shape factor can reflect the local slope of the freeform surface. The relationship between the shape factor ε_i and the local slope can be described by the following equation:

$$\varepsilon_i = k\frac{PV_i}{S_i}, \tag{2}$$

where, PV_i denotes the peak-to-valley value of the surface sag in unit i and S_i is the area of this unit. Coefficient k is related to the average shape factor specified in advance.

Fitting precision is an important indicator to assess the characterizing ability of a model. On account of the proportional relationship between the shape factor and the slope of every unit, the RBF-Slope model exhibits a different fitting feature to the RBF-Direct model. When fitting a surface with regions of different slopes, all the shape factors in the RBF-Direct model are set to one value. In the fitting of the sharp regions, the coefficients of the basis functions are adjusted to be larger than those in the flatter regions. Therefore, the basis functions in the sharp region can significantly influence the fitting of other regions in the aperture. In contrast, in the RBF-Slope model, the shape factors of the basis functions in sharp region are set to be larger than the shape factors in other regions to make these basis functions sharper, leading to reduced influence on the fitting of other regions in the aperture, thus yielding greater fitting precision. So the RBF-Slope model is more appropriate to fit surfaces with different slopes such as asymmetric surfaces. With greater fitting precision, the RBF-Slope model has better characterizing ability and is more efficient to eliminate aberration when characterizing asymmetric surfaces in optical system design.

3. Fitting for off-axis conic

In order to investigate the fitting abilities of the RBF-Direct and RBF-Slope models, we chose an off-axis conic in a rectangular aperture as the test example, which is an important application in optical systems operating in space. According to the first principle of the RBF-Slope model, the center distribution of this model is the same as that of the RBF-Direct model for a rectangular aperture; therefore, this test focuses on the effect of the second principle on the fitting performance of the RBF-Slope model. The vertex curvature radius of this conic was 455.4 mm and the conic constant was −1.306. The surface to be fitted was intercepted from the conic by a cube with side length of 110 mm. The distance between the center of the surface and the axis of the conic was 50 mm. The coordinate system used to characterize the surface is shown in Fig. 3(a). A centerline of the cube that was chosen to be normal to the surface at the intersection was specified as the z-axis. The x–y plane coincides with the tangent plane of the intersection. For this coordinate system, the sag of the off-axis conic is shown in Fig. 3(b). For the off-axis conic, the surface was symmetric about the x–z plane, and

Optics EXPRESS

thus the distribution of the shape factors decided by the slope had the symmetry shown in Fig. 3(c).

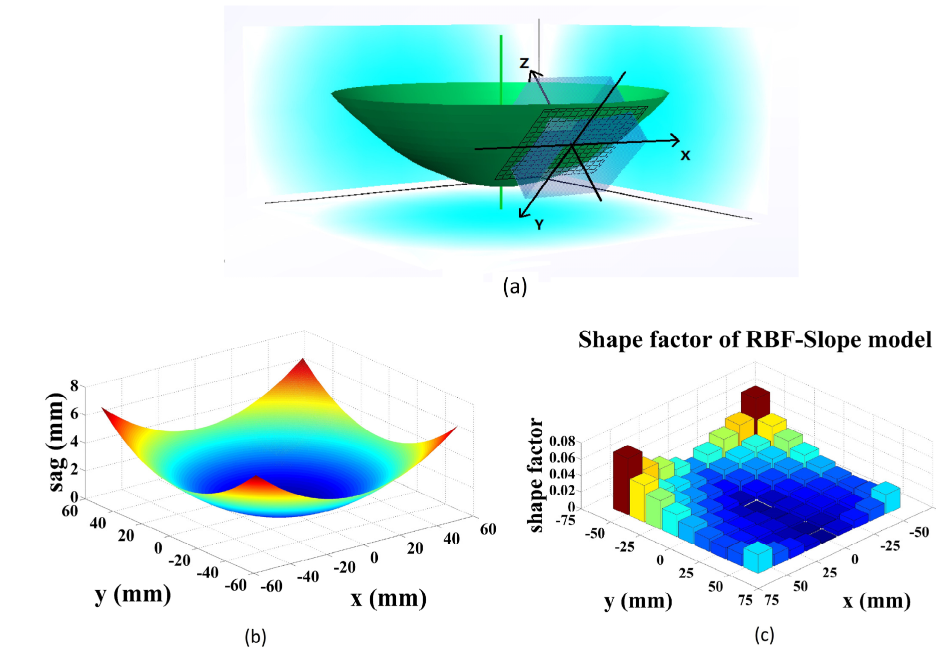

Fig. 3. (a) Coordinates to characterize off-axis conic, (b) off-axis conic in rectangular aperture, (c) shape factor of RBF-Slope model with number of basis functions = 81 and average shape factor = 0.008.

In our study, we used three different numbers of basis functions to fit this off-axis conic: 49, 64, and 81, for which there are 1849, 2500, and 3249 sample points respectively chosen to create the database. The sample points uniformly and regularly distribute in the aperture. Two models (RBF-Direct and RBF-Slope) with the average shape factor varying between 0.001 and 0.01 were used to fit this surface with least squares, and Householder transformation was used to deal with the ill-condition problems of least squares [18]. The fitting precision as evaluated by root mean square (RMS) errors and peak-to-valley (PV) errors values for different shape factors (for RBF-Direct model) or average shape factors (for RBF-Slope model) is shown in Figs. 4(a) and 4(b), respectively.

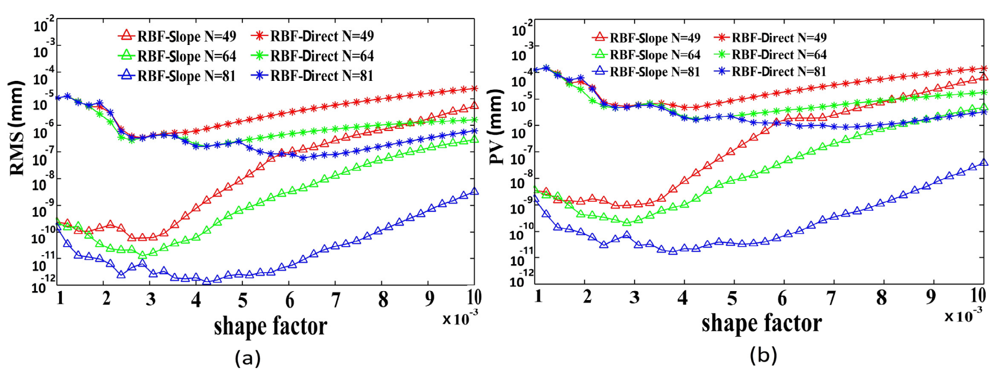

Fig. 4. (a) RMS errors and (b) PV errors of fitting for the off-axis conic when the RBF-Direct model and the RBF-Slope model are with 49, 64 and 81 basis functions respectively.

The results indicate that the fitting ability of the RBF-Slope model is better than that of the RBF-Direct model for the same number of basis functions, particularly for small shape factors ranging from 0.001 to 0.006. Because the distribution of the centers in these two models is the same in the rectangular aperture, the improvement of the precision can be completely attributed to the feature of the RBF-Slope model that the shape factor is decided by the surface slope, proving the improved characterizing ability of the RBF-Slope model for the off-axis conic. In addition, the result of the RBF-Slope model indicates that the fitting precision increases when the average shape factor reduces, which means that the RBF-Slope model with a smaller shape factor (flatter basis function) exhibits a higher fitting accuracy for a continuous surface with certain symmetry.

4. Fitting for paraboloid with bump

In order to compare the characterization abilities of the RBF-Direct model and the RBF-Slope model for large shape variation of a surface, we chose an F/1 paraboloid surface in a circular aperture added with three Gaussian functions as the test surface. The analytical expression of the surface is given as

$$z = \frac{(x^2 + y^2)}{80} + 0.05e^{-0.25[(x-7)^2+(y+6)^2]} + 0.6e^{-0.49[(x+3)^2+(y-2)^2]} + 0.03e^{-0.81[(x-5)^2+(y-7)^2]}, \quad (3)$$

This surface was formed by a paraboloid with three Gaussian functions. As the centers of these three Gaussian functions were close to each other, there is an obvious local variation on the paraboloid surface. The surface with the aperture normalized to 1 in terms of the radius is shown in Fig. 5(a). In addition to comparing the fitting precision of the two kinds of RBF models, we also considered the Zernike polynomial model to compare the characterization ability of the global polynomial model and the RBF models for this type of surface.

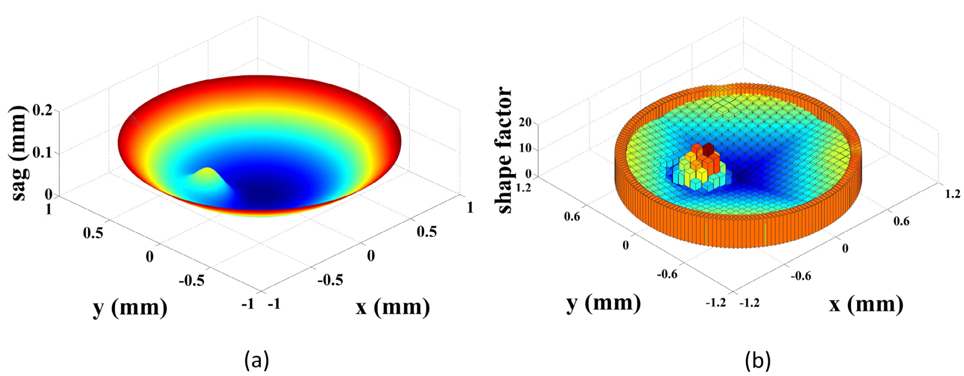

Fig. 5. (a) Sag of paraboloid with bump, (b) the shape factor of RBF-Slope model when the number of basis functions is 784 and the average shape factor is 5.

In order to accurately describe the sharp change of the surface, a large number of basis functions are needed to meet the precision requirement. Therefore, in our study, we teste 676, 729, and 784 basis functions to fit this paraboloid with a bump. There were 6000 sample points, the selection of which was based on the Halton sequence, chosen in the aperture to create the database. Three models, RBF-Direct, RBF-Slope and Zernike polynomial, were used to fit this surface with least squares solved by the Householder transformation. The shape factor of the RBF-Direct model and the average shape factor of RBF-Slope model were both set to 5, which is close to the optimal shape factor (or optimal average shape factor) values of two models in this fitting. The optimal shape factor (or optimal average shape factor) can be obtained by evaluating the fitting error of two models with the shape factor (or average shape factor) varying from 0 to 10. The fitting results of these models were listed in Table 1, and the fitting error of the models for 784 basis functions was shown in Figs. 6(a), 6(c), and 6(e). It can be seen that the fitting errors mainly existed on the edge of aperture. Considering the fitting effect for strong local variations (the bump) of the three models can't be clearly discriminated in the whole aperture, the fitting result within the 0.8 times the full aperture (the "0.8-aperture") for all three models was also provided in Table 1 and Figs. 6(b), 6(d), and 6(f) to show the fitting for the bump.

Table 1. Fitting results of parabolic surface with bump

	N	whole aperture		0.8 aperture	
		RMS (m)	PV (m)	RMS (m)	PV (m)
Gaussian RBF $\varepsilon = 5$	676	2.6144E-08	7.4876E-07	2.0923E-08	1.3149E-07
	729	1.4168E-08	3.7577E-07	1.1483E-08	9.5872E-08
	784	1.2511E-08	4.9058E-07	9.5772E-09	7.7042E-08
Gaussian RBF-Slope $\overline{\varepsilon} \approx 5$	676	7.7829E-10	2.3340E-08	8.0611E-10	1.0679E-08
	729	5.2223E-10	1.3217E-08	5.4119E-10	6.1580E-09
	784	4.6226E-10	2.5343E-08	4.3238E-10	5.2268E-09
Zernike Polynomial	676	4.0013E-08	5.6084E-06	7.2829E-09	9.9122E-08
	729	8.4325E-09	1.0021E-06	3.5316E-09	4.9530E-08
	784	5.7221E-09	6.7490E-07	2.3427E-09	3.3320E-08

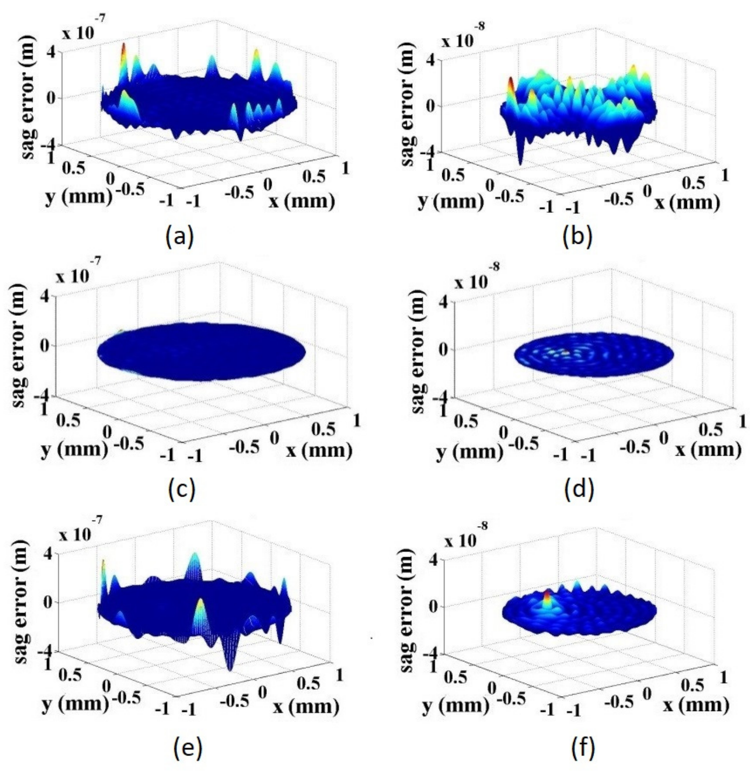

Fig. 6. Sag error in (a) whole aperture and (b) 0.8-aperture as fitted with RBF-Direct model with 784 basis functions, sag error in (c) whole aperture and (d) 0.8-aperture as fitted with RBF-Slope model with 784 basis functions, and sag error in (e) whole aperture and (f) 0.8-aperture fitted with Zernike polynomial with 784 basis functions.

Optics EXPRESS

The results show that the fitting accuracy of the RBF-Slope model is higher than those of the other two models for the 0.8-aperture, which proves the fitting ability of the RBF-Slope model in strongly varying regions of the surface. Furthermore, the RBF-Slope model also exhibits a better fitting performance over the whole aperture. When fitting with the RBF-Direct model, uniform shape factors over the whole surface limit the fitting precision for the target surface. As can be observed from Figs. 6(a) and 6(b), the RBF-Direct model cannot achieve a good fitting precision for either the whole aperture or the 0.8-aperture. The Zernike polynomial model is also not suitable to characterize surfaces with strong regional surface variations because of its global feature. As can be observed in Figs. 6(e) and 6(f), compared with other regions, the edge and the bump of the surface have obviously larger fitting errors. When fitting with the RBF-Slope model, the shape factors of the basis functions locating near to the edge and the bump of surface are larger, which is illustrated in Fig. 5. With stronger locality of the basis function in these areas, these bases could accurately fit the local variation while negligibly affecting other parts of the surface. Therefore, for this type of surface, the characterization ability of the RBF-Slope model is better than that of the RBF-Direct and Zernike polynomial models, as indicated in Figs. 6(c) and 6(d).

5. Design of a single mirror magnifier

After investigating the fitting ability of the RBF-Slope model, we applied the two RBF models (RBF-Slope and RBF-Direct) to the design of a single mirror magnifier to test the optical performance of the two models. A single mirror magnifier is the simplest structure for head-worn display (HWD) and the color correction is not required [16]. In our design of the single mirror magnifier system, the single mirror was represented by a Gaussian RBF model (the number of basis functions is set to 64 in both models). The design parameters and the achieved values were listed in Table 2, most of which are identical to the corresponding design values provided in [16]. It is can be seen from Fig. 1(a) that the symmetry plane of the geometry in [16] was shown as XZ plane. For a better comparison, the XZ plane was also set to the plane of symmetry in our design. Figure 7 illustrates the flow diagram of the design method.

Table 2. Parameters and achieved values of single mirror magnifier

Parameter	Achieved value
Exit pupil diameter (mm)	3
Effective focal length (mm)	14.25
Full diagonal field of view	24°
Working wavelength	587.56 nm
Distortion	<10%

Optics EXPRESS

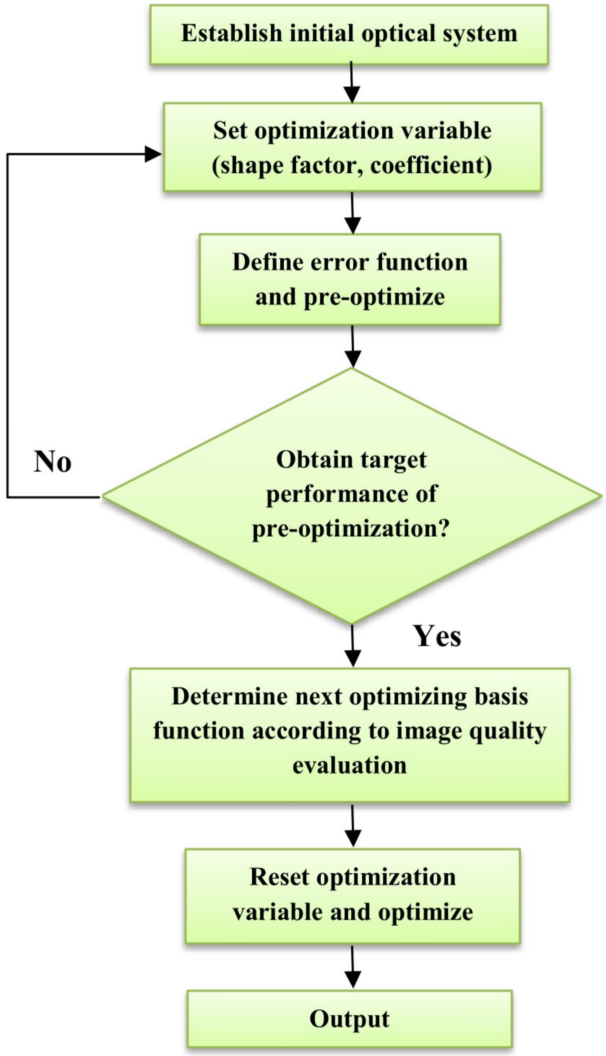

Fig. 7. Flow diagram of the optical design process.

Before establishing the initial system with RBF-Slope model, a conic was used to represent the mirror surface to roughly determine the aperture of the surface. Then the conic was fitted by RBF-Slope model so that the initial optical system of RBF-Slope model was established. The initial system of RBF-Direct model was also established by fitting the conic. For a comparison with the design in [16], the average shape factor of RBF-Slope model as well as the shape factor of RBF-Direct model was set to 0.707, which is the value of shape factor of RBF model applied in the optical design in [16]. Next, we set the parameters of the basis functions as variables and performed the optimization.

Figure 8 shows the RMS wavefront error (WFE) of the system designed with the RBF-Slope model after pre-optimization. It is obvious that the RMS WFE of the FOV circled with the blue line is significantly larger than the RMS WFE of other FOVs, and then we only considered the basis functions corresponding to these areas in the next optimization. After ray tracing of the FOV specified by the blue line, we obtained the corresponding coordinates on the mirror surface of these FOVs (listed in Table 3). Subsequently, the centers of the basis

Optics EXPRESS

functions around these FOVs could be easily determined. Next, the shape factors and the coefficients of these basis functions were set as variables in next optimization process. Finally, the next optimization was performed and the final design was generated.

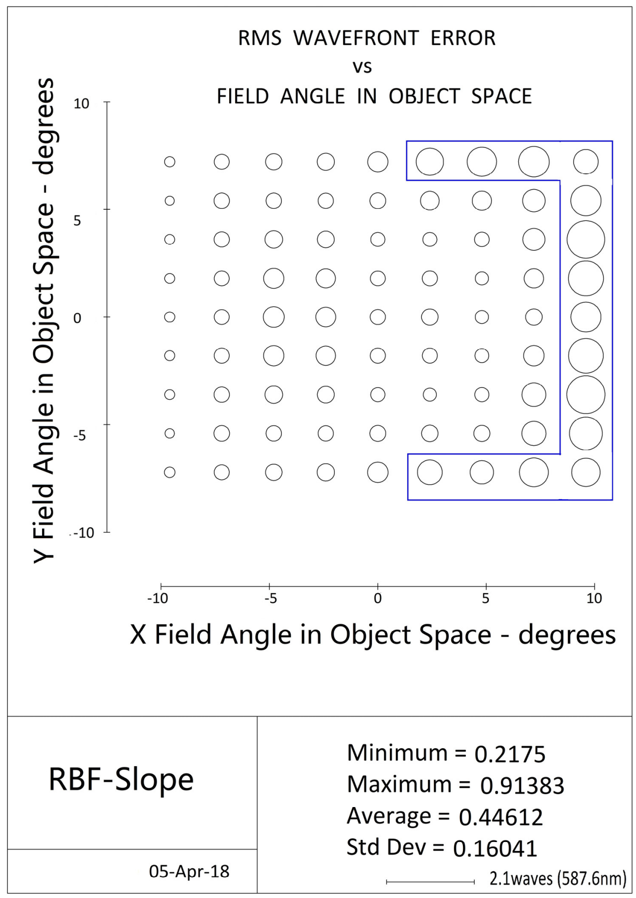

Fig. 8. Root mean square (RMS) wavefront error (WFE) in the full field of view (FOV) of the system when RBF-Slope model was applied.

Table 3. Specified fields of view (FOVs) and corresponding coordinates

FOV	X coordinate	Y coordinate	Z coordinate
(0°,7.2°)	−0.40341	2.15582	0.25317
(0°,-7.2°)	−0.40353	−2.15588	0.25261
(4.8°,7.2°)	1.07579	2.18946	0.21752
(4.8°,-7.2°)	1.07570	−2.18962	0.21705
(9.6°,7.2°)	2.59289	2.21406	0.10077
(9.6°,-7.2°)	2.59282	−2.21428	0.10027
(9.6°,3.6°)	2.61877	1.10700	0.16685
(9.6°,-3.6°)	2.61873	−1.10722	0.16658
(9.6°,0°)	2.62740	−0.00011	0.18885

Figure 9(a) illustrates the shape factors of the basis functions over the whole surface (the green plane represents the shape factor value of the RBF-Direct model). It can be observed that the shape factors of the area when X > 0 are larger than those when X < 0. Over the whole surface, the largest shape factor is about 21 times the smallest shape factor. The final surface shape was shown in Figs. 9(b) and 9(c). It is obvious that the slope in the X > 0 area is larger than the slope in the X < 0 area, corresponding to the distribution of shape factors.

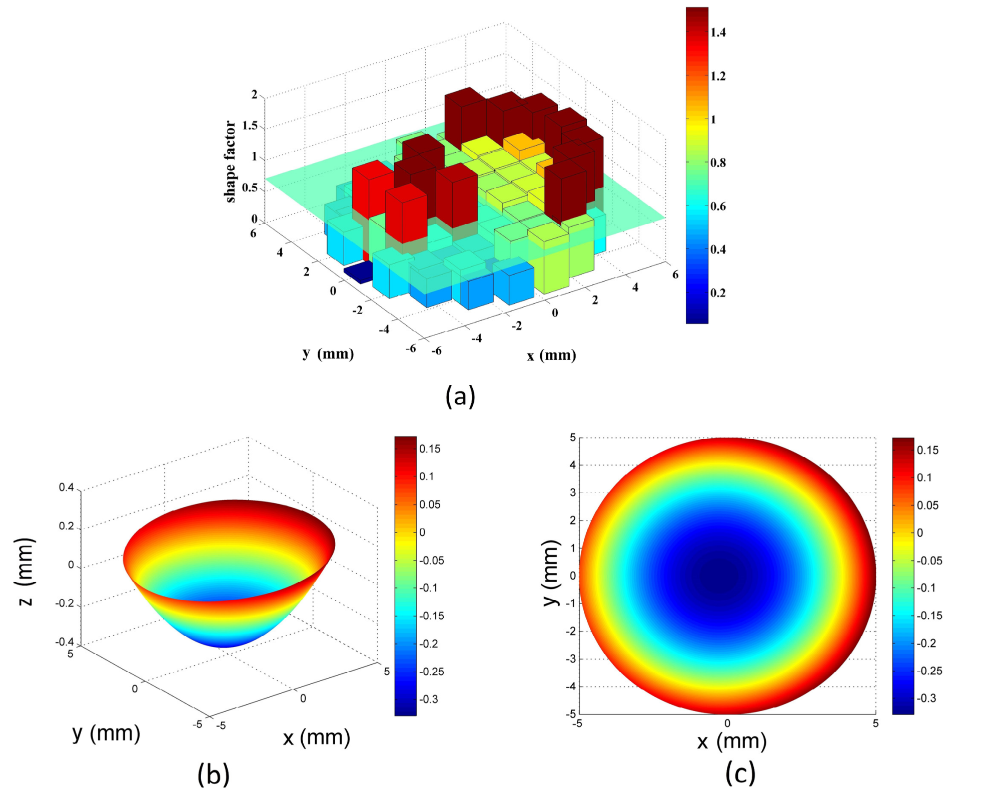

Fig. 9. (a) Shape factors of basis functions over the whole surface. (b) Surface shape of mirror represented by RBF-Slope model. (c) Surface of the mirror represented by RBF-Slope model in X–Y plane.

Figure 10 illustrates the final 2D and 3D layouts of the single mirror magnifier represented by the RBF-Slope model, and the optical performances of the two models are tabulated in Table 4. The modulation transfer function (MTF) at 23 cycles/mm and RMS WFE in the full FOV for the two models were plotted in Figs. 11 and 12, respectively.

From Fig. 11, we noted that the MTF is obviously increased with the RBF-Slope model in the $X > 0$ FOV than with the RBF-Direct model. Meanwhile, the decrease of RMS WFE in the $X > 0$ FOV is also obvious in Fig. 12. The changeable shape factor of the RBF-Slope model plays the most important role in the improvement of aberration balancing. Overall, the RBF-Slope model demonstrates a better design result in terms of distortion control, MTF and RMS WFE over the full FOV than the RBF-Direct model in the design of the single mirror magnifier system. Thus, our results prove that the RBF-Slope model satisfies the design demands of a single mirror magnifier and can achieve better optical performance than the RBF-Direct model.

Research Article Vol. 26, No. 11 | 28 May 2018 | OPTICS EXPRESS 14022
Optics EXPRESS

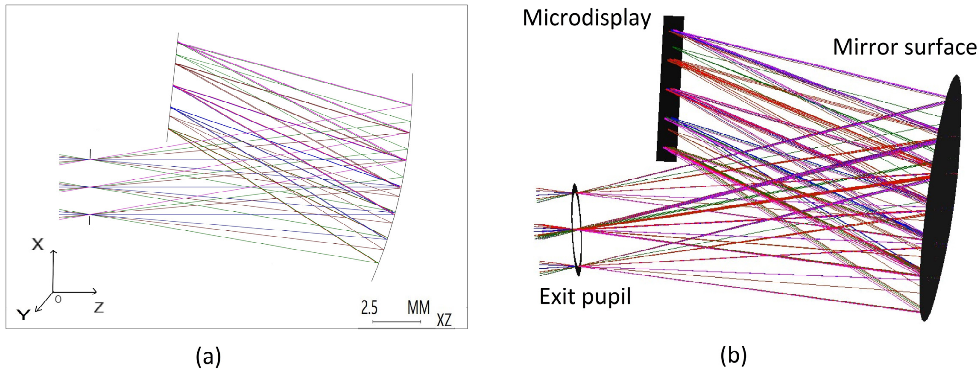

Fig. 10. (a) 2D layout and (b) 3D layouts of single mirror magnifier.

Table 4. Comparison of optical performance of the two radial basis function models considered in the study

Model	Diffraction sine wave MTF (23 cycles/mm)	Max Distortion	RMS WFE
RBF-Direct	0.48543	4.38	0.58327λ
RBF-Slope	0.59926	3.39	0.43613λ

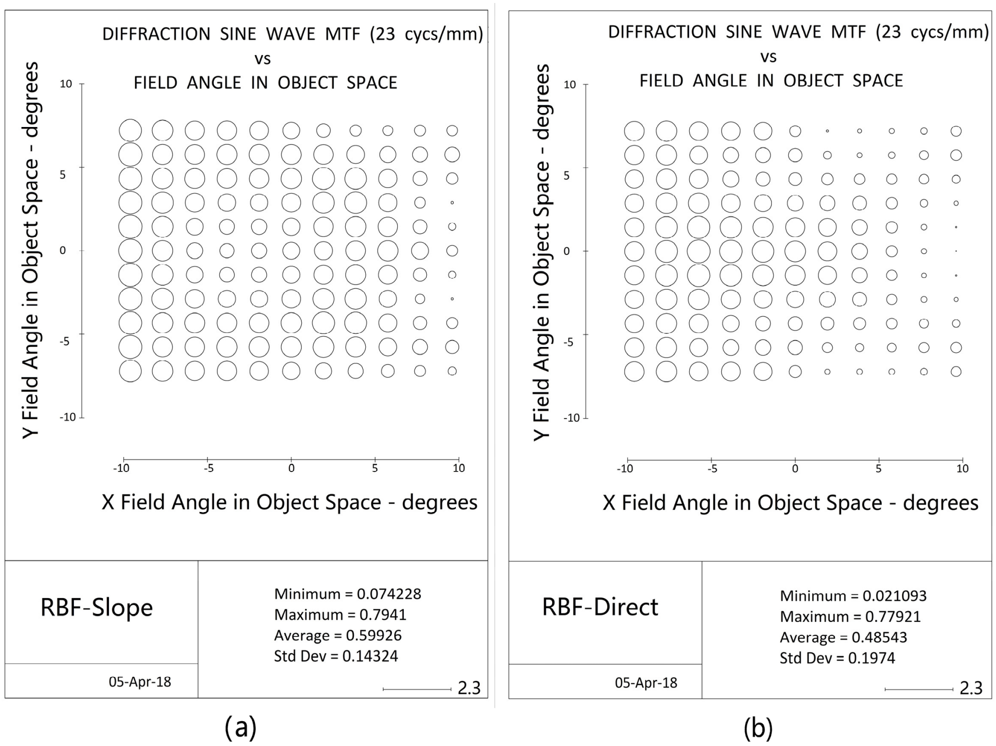

Fig. 11. Modulation transfer function (MTF) in the full field of view (FOV) of the optical system with application of (a) the RBF-Slope model and (b) the RBF-Direct model.

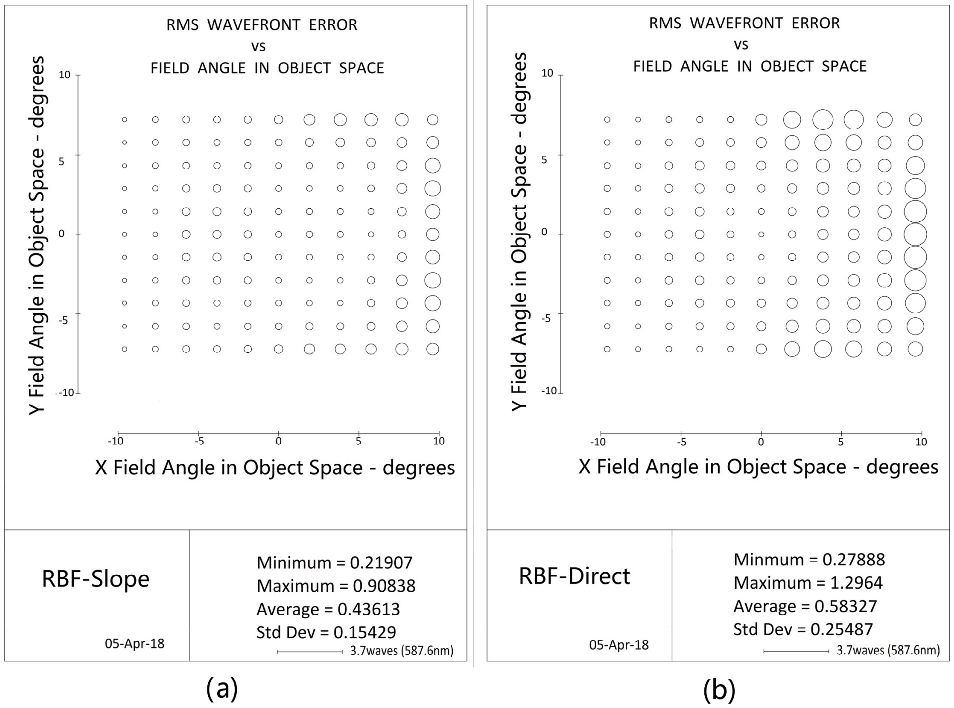

Fig. 12. Root mean square (RMS) wavefront error (WFE) in the full field of view (FOV) of the optical system upon applying (a) the RBF-Slope model and (b) the RBF-Direct model.

6. Conclusion

In this paper, we proposed a new type of model for the characterization of freeform optical surfaces, which we called the RBF-Slope model. Based on the RBF-Direct model, the RBF-Slope model improves the distribution of the basis functions and establishes the relationship between the shape factor and local surface slope. The results of fitting an off-axis conic and a paraboloid with a bump showed that the precision of the RBF-Slope model was one to two orders in magnitude higher than that of the RBF-Direct model. In the design of a single mirror magnifier, the results indicated that the optical performance of the RBF-Slope model was better than that of the RBF-Direct model and the performance depended on the shape factor when the basis-function number was fixed. In future, we plan to further improve on the RBF-Slope model and attempt to apply this model to design different optical systems.

Funding

National Natural Science Foundation of China (NSFC) (11474169, 61675100, 61575097); Tianjin Natural Science Foundation (15JCYBJC16900); Science and Technology Innovation Program of the Chinese Academy of Sciences.